NEAR-THRESHOLD CORRELATIONS OF NEUTRONS*

J. Okołowicz

The H. Niewodniczański Institute of Nuclear Physics, Polish Academy of Sciences
Radzikowskiego 152, 31-342 Kraków, Poland

W. Nazarewicz

Department of Physics and Astronomy, University of Tennessee
Knoxville, Tennessee 37996, USA
Physics Division, Oak Ridge National Laboratory
Oak Ridge, Tennessee 37831, USA
Institute of Theoretical Physics, University of Warsaw
Hoża 69, 00-681 Warszawa, Poland

M. Płoszajczak

Grand Accélérateur National d'Ions Lourds (GANIL)
CEA/DSM — CNRS/IN2P3, BP 55027, 14076 Caen Cedex, France

(Received December 16, 2013)

The emergence of charged-particle clustering in near-threshold configuration is a phenomenon which can be explained in the Open Quantum System (OQS) description of the atomic nucleus. In this work, we apply the realistic Shell Model Embedded in the Continuum (SMEC) to elucidate emergence of neutron correlations in near-threshold many-body states coupled to $\ell = 1, 2$ neutron decay channels. Consequences of continuum coupling for spectra and the emergence of complex multi-neutron correlations are briefly discussed.

DOI:10.5506/APhysPolB.45.331
PACS numbers: 25.70.Ef, 03.65.Vf, 21.60.Cs, 25.40.Cm

1. Introduction

It was argued recently that the emergence of charged particle clustering in near-threshold configurations is a genuine consequence of continuum

* Presented at the XXXIII Mazurian Lakes Conference on Physics, Piaski, Poland, September 1–7, 2013.

coupling in the OQS description of nuclear many-body system [1]. The coupling of Shell Model (SM) eigenstates via the particle decay channel leads to the formation of the aligned OQS eigenstate which captures most of the continuum coupling and is an archetype of the cluster state. The collectivity of this state is a signature of the instability in an ensemble of all SM states having the same quantum numbers and coupled to the same decay channel.

What can be said about the nature and appearance of the (multi-)neutron correlations in near-threshold states? The N- and Z-dependence of the nuclear binding energy rules out the existence of stable like-particle clusters. An interplay between nuclear mean field and pairing correlations determines the ordering of like-particle decay thresholds and excludes *e.g.* the appearance of $4n$-decay channel below the $2n$-decay channel. Hence, the complex clusters composed of like nucleons can be seen only as dynamical short-lived resonance structures.

In this paper, we shall analyze properties of the SMEC wave functions to understand the modification of spectrum of SM eigenvalues by the coupling to the $\ell = 1, 2$ neutron decay threshold. The configuration mixing in near-threshold SMEC states will be illustrated by studying exceptional points (EPs) of the complex-extended SMEC Hamiltonian. By investigating the energy- and (complex) interaction-dependence of EPs around the neutron emission threshold, we hope to reveal generic features of the clusterization mechanism for neutrons and its sensitivity to the angular momentum ℓ involved in the neutron decay channel.

2. SMEC: Shell Model for Open Quantum Systems

SMEC, which provides a unified description of structure and reactions with up to two nucleons in the scattering continuum [2], describes many-body states of an OQS using the effective non-Hermitian Hamiltonian [3, 4]. The configuration mixing due to the competition between Hermitian and anti-Hermitian terms in the effective Hamiltonian is a source of collective features such as, *e.g.*, the resonance trapping [5–7] and super-radiance phenomenon [8, 9], multichannel coupling effects in reaction cross-sections [10], and charge-particle clustering [1].

The detailed description of SMEC can be found elsewhere [3, 7]. The Hilbert space in this approach is divided into orthogonal subspaces $\mathcal{Q}_\mu$, where index μ denotes the number of particles in the scattering continuum. An OQS description of internal dynamics in $\mathcal{Q}_0$ includes couplings to the environment of decay channels, and is modelled by the energy-dependent Hamiltonian

$$\mathcal{H}(E) = H_0 + H_1(E) = H_0 + V_0^2 h(E)\,. \tag{1}$$

In this expression, H_0 is the Closed Quantum System (CQS) Hamiltonian (the SM Hamiltonian), V_0 is the continuum-coupling strength, E is the scattering energy, and $h(E)$ is the coupling term between localized states in $\mathcal{Q}_0$ and the environment of decay channels. The 'external' mixing of any SM eigenstates due to $H_1(E)$ consists of the Hermitian principal value integral describing virtual excitations to the continuum and the anti-Hermitian residuum which represents the irreversible decay out of the internal space $\mathcal{Q}_0$.

The SMEC solutions in $\mathcal{Q}_0$ are found by solving the eigenproblem for the non-Hermitian Hamiltonian (1). The eigenstates $|\Phi_j\rangle$ of $\mathcal{H}$ are mixtures of SM eigenstates $|\psi_i\rangle$. The continuum-coupling correlation energy of the SM eigenstate $|\psi_i\rangle$,

$$E_{\mathrm{corr};i}(E) = \langle\psi_i|\mathcal{H} - H_0|\psi_i\rangle \simeq V_0^2\langle\psi_i|h(E)|\psi_i\rangle\,, \tag{2}$$

depends on the structure of the SM eigenstate and the nature of the decay channel. In general, the continuum coupling lowers the binding energies of eigenstates that are close to the decay threshold. The peak of the continuum coupling correlation energy can be shifted above the threshold due to a combined effect of the centrifugal and Coulomb barriers.

The information about the configuration mixing is contained in the double poles of the scattering matrix, the so-called exceptional points (EPs) [11]. The mixing of wave functions in CQSs is related to nearby EP(s) of the complex-extended CQS Hamiltonian. Similarly, in OQSs one should analyze the distribution of EPs of the complex-extended OQS Hamiltonian [12]. Since the OQS Hamiltonian (1) is energy dependent, the complete picture of the near-threshold configuration mixing is contained in exceptional threads, ETs, the trajectories of coalescing eigenvalues $E_{i_1}(E) = E_{i_2}(E)$ of the effective Hamiltonian for a complex value of V_0 [13].

3. Continuum-coupling correlations near the neutral particle decay channel

It was shown in Ref. [1] that the continuum-coupling correlations may lead to the collective rearrangements involving many SM eigenstates, *i.e.* to instability of certain SM eigenstates near the charge particle decay threshold. In this section, we shall discuss these effects on the example of $J^\pi = 0^+$ SM eigenstates coupled to the one-neutron decay channel in $\ell = 1, 2$ partial waves.

3.1. Continuum coupling correlation energy

Figure 1 shows a typical shape of the continuum-coupling correlation energy (2) for four SM states that are coupled to the $\ell = 2$ neutron decay channel. The SMEC calculations for ^{20}O have been carried out in the

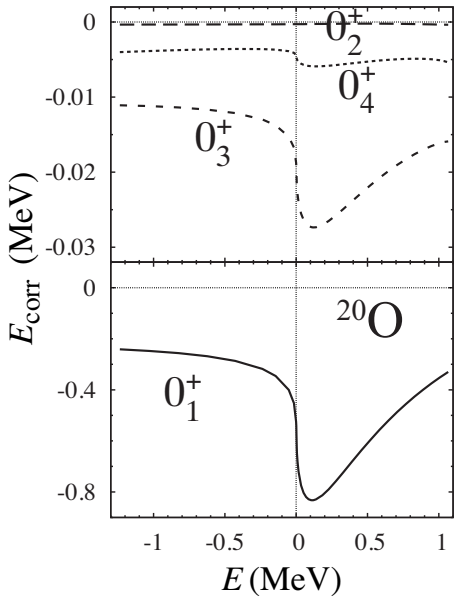

Fig. 1. The continuum-coupling correlation energy $E_{\rm corr}$ to the four lowest $J^\pi = 0^+$ shell model eigenvalues in ^{20}O as a function of the neutron energy E. The lower panel shows $E_{\rm corr}$ to the ground state wave function 0^+_1 (the solid line). The upper panel presents $E_{\rm corr}$ to 0^+_2 (the dashed line), 0^+_3 (the dotted line), and 0^+_4 (the long-dashed line) shell model wave functions. The neutron threshold $^{19}{\rm O}(5/2^+) + n(\ell = 2)$ at $E = 0$ is indicated by a vertical dotted line.

$0d_{5/2}, 1s_{1/2}, 0d_{3/2}$ SM model space. For H_0, we take the USDB Hamiltonian [14]. The residual coupling between $\mathcal{Q}_0$ and the embedding one-neutron continuum is generated by the contact force with the continuum coupling strength $V_0 = -1000$ MeV fm^3. The correlation energy is proportional to V_0^2 and to the average density of SM states around the threshold. An interplay between the centrifugal potential and the continuum coupling determines the peak of the continuum coupling correlation energy, *i.e.*, the full width at half maximum σ and the centroid $E_{\rm TP}$ of the correlation energy around the maximum.

The continuum coupling correlation energy rapidly decreases for excited states. The lowest energy eigenvalue shows pronounced dependence on the continuum coupling in the vicinity of the threshold. The minimum is shifted above the threshold by about 0.15 MeV due to the $\ell = 2$ centrifugal barrier. The width σ of the correlation energy peak is about ~ 0.5 MeV, similarly to a typical value of σ in the case of coupling to the $\ell = 0$ charged-particle emission threshold.

The near-threshold effects of the continuum coupling on SMEC eigenvalues depend strongly on the angular momentum ℓ. Figure 2 shows the dependence of four lowest 0^+ eigenvalues of SMEC in ^{16}C on the neutron energy due to the coupling to the neutron decay channel in the partial wave $\ell = 1$. The SMEC calculations for ^{16}C have been carried out in the $0p_{1/2}, 0d_{5/2}, 1s_{1/2}$ SM model space. For H_0 in this case, we take the ZBM2C Hamiltonian [15]. The residual continuum coupling is generated by the contact force with the strength $V_0 = -1000$ MeV fm^3.

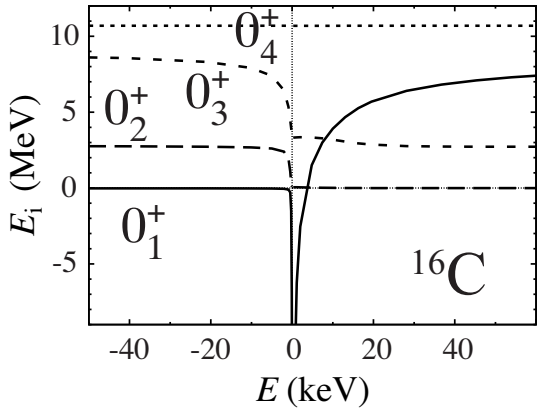

Fig. 2. Energies E_i of the four lowest $J^\pi = 0^+$ eigenvalues of the effective Hamiltonian (1) for ^{16}C as a function of the neutron energy E. The neutron threshold $^{15}\mathrm{C}(1/2^-) + n(\ell = 1)$ at $E = 0$ is indicated by a vertical dotted line.

One may notice a successive avoided crossings of SMEC eigenvalues indicating strong mixing. For the lowest eigenvalue, the variation of energy around the neutron emission threshold $^{15}\mathrm{C}(1/2^-) + n(\ell = 1)$ is restricted to a range of only few keV. In this narrow energy range, the SMEC eigenvalue has a singular cusp and the width of the correlation energy peak is less than ~ 1 keV. In this energy interval, all excited 0^+ states are pushed up high in energy with respect to the aligned state 0^+_1. The singular energy behaviour in the vicinity of the threshold is less visible for higher eigenvalues and the width of the correlation energy peak is also broader.

3.2. Configuration mixing near the neutron emission threshold

Comprehensive picture of the near-threshold configuration mixing in SMEC wave functions can be obtained by investigating properties of the ETs of the complex-extended SMEC Hamiltonian [1]. The anti-Hermitian mixing leads to the collectivization of SM eigenstates and the accumulation of collective effects in a single many-body state close to the particle-emission

threshold. Such a state of the OQS, the so-called 'aligned state', couples strongly to the decay channel and exhausts most of the total continuum-coupling correlation energy. The energy dependence of ETs in a vicinity of the threshold is shown in Fig. 3 for eigenstates of ^{20}O coupled to the channel $^{19}\mathrm{O}(5/2^+) + n(\ell = 2)$, and in Fig. 4 for eigenstates of ^{16}C coupled to the channel $^{15}\mathrm{C}(1/2^-) + n(\ell = 1)$. We consider four 0^+ SM eigenstates and, hence, six different ETs for decaying resonances. All ETs which are relevant for the collective mixing of SM states involve the aligned eigenstate 0^+_1. They exhibit a minimum of $|V_0|$ (the turning point, TP) at the same neutron energy. At this energy, the collective mixing of SM states is maximal. The remaining ETs are found at exceedingly large values of $|V_0|$ (see the upper

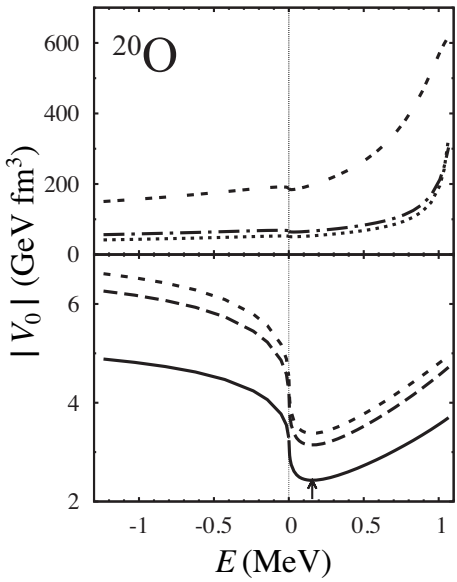

Fig. 3. Exceptional threads $|V_0|(E)$ for the 0^+ eigenvalues of the complex-extended SMEC Hamiltonian (1) in ^{20}O. Only exceptional threads corresponding to decaying resonances are shown. Each point along an exceptional thread is an exceptional point labelled by the neutron energy with respect to the $^{19}\mathrm{O}(5/2^+) + n(\ell = 2)$ threshold. There are six threads in this case. Three of them (bottom panel), involving the aligned 0^+_1 state, are found in the physical range of $|V_0|$ values and correspond to a coalescence of $0^+_1 - 0^+_2$ (solid line), $0^+_1 - 0^+_3$ (long-dashed line), and $0^+_1 - 0^+_4$ (short-dashed line) eigenvalues. The remaining three threads (top panel), $0^+_2 - 0^+_3$, $0^+_2 - 0^+_4$, and $0^+_3 - 0^+_4$, correspond to very large values of $|V_0|$ and have no influence on the mixing of shell model eigenstates. The arrow indicates the turning point of the exceptional thread corresponding to the maximal continuum coupling. For more details, see the description in the text.

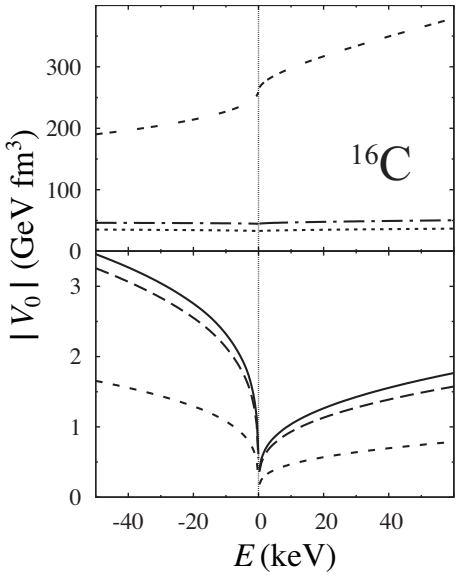

Fig. 4. The same as in Fig. 3 but for ^{16}C shell model eigenstates coupled to the neutron decay channel $^{15}\mathrm{C}(1/2^-) + n(\ell = 1)$. For more details, see the caption of Fig. 3 and a discussion in the text.

panel in Figs. 3 and 4) and have no influence on the configuration mixing. In the case of ^{20}O, the turning point energy $E_{\mathrm{TP}} \simeq 0.18$ MeV is above the $\ell = 2$ neutron emission threshold. The dependence of $|V_0|(E)$ around the turning point for those ETs which involve the eigenstate 0^+_1 is asymmetric and significant configuration mixing in SMEC wave functions is expected up to $E \simeq 1.2$ MeV.

In the case of ^{16}C, the turning point is seen at the $\ell = 1$ neutron emission threshold for all ETs containing the aligned eigenstate 0^+ SM. The energy dependence in the vicinity of the threshold of these ETs takes a form of the cusp.

Another view on the configuration mixing around the neutron decay threshold is provided in Figs. 5 and 6, which show the ETs in the complex-V_0 plane for the 0^+ states coupled to $\ell = 2$ and $\ell = 1$ neutron decay channels, respectively. Each ET in these figures involves the aligned state 0^+_1 and each point on every trajectory in the complex-V_0 plane corresponds to a different neutron energy.

In Fig. 5, one can see that the pattern of most important ETs involving the aligned state 0^+_1 has two cardinal points: the threshold which is denoted by a circle, and the turning point which is the point of the closest approach of the ET to the real-V_0 axis. At the threshold $E = 0$, the real part of the

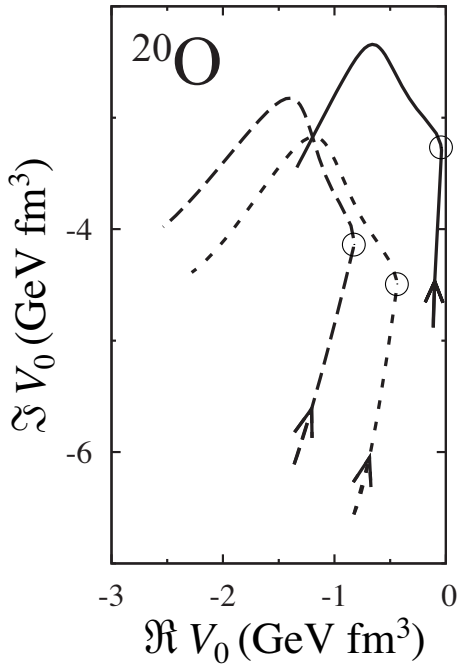

Fig. 5. Exceptional threads in the complex-V_0 plane for 0^+ eigenfunctions of the SMEC Hamiltonian in ^{20}O coupled to $\ell = 2$ neutron decay channel $^{19}\mathrm{O}(5/2^+) + n(\ell = 2)$. Each point at the exceptional thread corresponds to an exceptional point at a definite energy E. The threshold position ($E = 0$) is indicated with a circle for each thread. Only the exceptional threads formed by a coalescence of $(0_1^+$–$0_2^+)$ (solid line), $(0_1^+, 0_3^+)$ (long-dashed line), and $(0_1^+, 0_4^+)$ (dashed line) eigenvalues of decaying resonances at low values of $|V_0|$ are shown. Arrows indicate the way in which neutron energies increase.

continuum coupling constant for each ET is closest to the axis $\mathcal{R}eV_0 = 0$. For $< 0E < E_{\mathrm{TP}}$, the real part of V_0 begins to move away from the axis $\mathcal{R}eV_0 = 0$, whereas the imaginary part of V_0 continues to approach rapidly the real-V_0 axis ($\mathcal{I}mV_0 = 0$). As a result, the strongest collectivization of SM eigenstate and, consequently, the largest continuum-coupling energy correction for $\ell = 2$ takes place at the turning point and not at the neutron emission threshold. For energies above the turning point, both $|\mathcal{R}eV_0|$ and $|\mathcal{I}mV_0|$ increase monotonously and the collectivization of SM eigenstates disappears gradually.

The radical change of the pattern appears when changing the angular momentum involved in the neutron emission channel from $\ell = 2$ (Fig. 5) to $\ell = 1$ (Fig. 6). In this case, the whole segment of ETs, in between

$E = 0$ and $E = E_{\rm TP}$, disappears and the turning point coincides with the neutron emission threshold. One can see that for energies below the threshold, all ETs which involve the aligned state tend to the point $\mathcal{R}eV_0 = 0$, $\mathcal{I}mV_0 = 0$, what is another signature of the extreme collectivization of the aligned SMEC eigenstate in this case. Above the threshold, both $|\mathcal{R}eV_0|$ and $|\mathcal{I}mV_0|$ increase rapidly with increasing neutron energy and all effects of the coupling of SM eigenstates through the decay channel cease to exist.

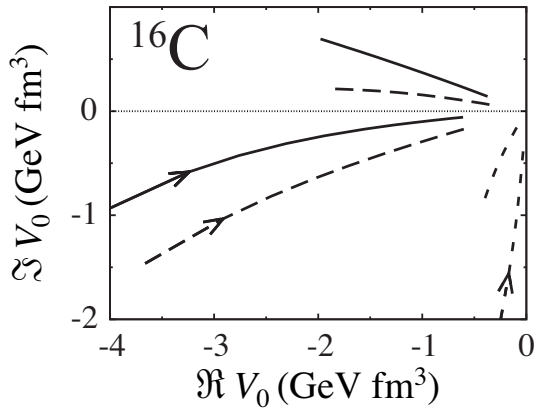

Fig. 6. The same as in Fig. 5 but for ^{16}C SMEC eigenfunctions coupled to the neutron decay channel $^{15}\mathrm{C}(1/2^-) + n(\ell = 1)$. For more details, see the caption of Fig. 5 and a discussion in the text.

We assert that the collective mixing of SM eigenstates via the aligned state is the origin of strong multi-neutron correlations in near-threshold states. For multi-neutron configurations, the observation of clustering depends on whether *(i)* a SM state is inside of the opportunity energy window given by the competition between the continuum coupling and the centrifugal potential, and *(ii)* its lifetime is sufficiently long to be detected. For SM states coupled to the cluster decay channel in low partial waves ($\ell = 0, 1$), the window of opportunity for multi-neutron clustering is situated in a narrow energy range around the turning point at the multi-neutron decay threshold. For higher partial waves ($\ell \geq 2$), this energy window moves above the multi-neutron decay threshold but an experimental observation of neutron clusters is compromised by the rapid decrease of lifetime of such configurations.

4. Conclusions

The existence of multi-neutron clustering is an old problem of low-energy nuclear physics. Recently, this problem has been revived by Marqués *et al.* [16] who reported the observation of neutron clusters in the disintegration

of beryllium and lithium nuclei. It was claimed that observed correlated four neutrons in disintegration of ^{14}Be could be related to four neutron halo in this nucleus. This report spurred many theoretical works which rejected the existence of bound tetraneutron as incompatible with our understanding of nuclear forces [17] (see, however, a discussion in Ref. [18] of a two-dineutron molecule). The isospin structure of the nuclear force prevents the existence of stable nuclei made of like nucleons. It also explains the energetic order of decay channels, *e.g.* ensures that a $4n$-emission threshold is above $2n$- and/or $1n$-emission thresholds. However, the nature of nuclear forces does not preclude the manifestation of tetraneutron correlations in the vicinity of the $4n$-emission threshold. The tetraneutron clustering may arise as a consequence of the collective coupling of many-body resonances via the $4n$-emission channel. Since at energies close to the $4n$-emission channel both $1n$- and $2n$-emission channels are opened, the tetraneutron correlations can be influenced by the coupling to these channels as well.

The mechanism responsible for the creation of multi-neutron cluster states is analogous to the formation mechanism of charged clusters and involves the aligned near-threshold state. The absence of stable multi-neutron clusters/nuclei is the only difference between, *e.g.* the dineutron decay from the 3α-decay of a Hoyle state in ^{12}C. Manifestations of the collective nature of the aligned state depend on the strength of the continuum coupling, the density of SM states, the structure of the emission channel, and the energy of the aligned state relative to the threshold. For $\ell = 1$ neutron decay channel, the collectivity of the aligned state is directly related to the increase of the energy gap between the aligned state and the higher excited states with the same quantum numbers. For channels with higher angular momenta ($\ell \geq 2$), the optimal energy window for the formation of the collective multi-neutron state is pushed above the decay threshold and the collectivity of this state is significantly reduced.

We have demonstrated that the point of maximum continuum coupling energy is related to the turning point of all ETs involving the aligned state. By construction, the turning point does not depend on the continuum-coupling strength. This point coalesces with the emission threshold for SM states coupled to $\ell = 1$ neutron decay channels.

The maximum of continuum coupling correlation energy is weakly dependent on the continuum-coupling strength, and the mass of both emitter and emitted particle. Hence, contrary to the charged-particle clustering, which is predicted to disappear in heavier nuclei, the multi-neutron correlations around the $\ell = 1$ multi-neutron decay threshold should survive in the whole chart of nuclei. However, the presence of these strong correlations is expected only in the narrow range of energies around the threshold which makes their experimental detection difficult. The closest approxima-

tion to a genuine multi-neutron cluster states are $2n$-halo states. However, the $2n$-separation energy in all experimentally studied cases is too large to speak about a truly dineutron cluster configuration [19]. The experimental observation of heavier multi-neutron clusters in the vicinity of the corresponding emission threshold remains a challenging open question for future studies.

This work was supported in part by the Ministry of Science and Higher Education (MNiSW) grant No. N N202 033837, the Collaboration COPIN–GANIL on physics of exotic nuclei, the Project SARFEN (Structure And Reactions For Exotic Nuclei) within the framework of the ERANET NuPNET, FUSTIPEN (French–U.S. Theory Institute for Physics with Exotic Nuclei) under DOE grant number DE-FG02-10ER41700, and by the DOE grant DE-FG02-96ER40963 with the University of Tennessee.

REFERENCES

[1] J. Okołowicz, M. Płoszajczak, W. Nazarewicz, *Prog. Theor. Phys. Suppl.* **196**, 230 (2012); J. Okołowicz, W. Nazarewicz, M. Płoszajczak, *Fortschr. Phys.* **61**, 66 (2013).

[2] K. Bennaceur, F. Nowacki, J. Okołowicz, M. Płoszajczak, *Nucl. Phys.* **A651**, 289 (1999); J. Rotureau, J. Okołowicz, M. Płoszajczak, *Nucl. Phys.* **A767**, 13 (2006).

[3] J. Okołowicz, M. Płoszajczak, I. Rotter, *Phys. Rep.* **374**, 271 (2003).

[4] A. Volya, V. Zelevinsky, *Phys. Rev.* **C74**, 064314 (2006).

[5] P. Kleinwachter, I. Rotter, *Phys. Rev.* **C32**, 1742 (1985); I. Rotter, *Rep. Prog. Phys.* **54**, 635 (1991).

[6] V.V. Sokolov, V.G. Zelevinsky, *Phys. Lett.* **B202**, 10 (1988); *Nucl. Phys.* **A504**, 562 (1989).

[7] S. Drożdż, J. Okołowicz, M. Płoszajczak, I. Rotter, *Phys. Rev.* **C62**, 24313 (2000).

[8] R.H. Dicke, *Phys. Rev.* **93**, 99 (1954).

[9] N. Auerbach, V.G. Zelevinsky, *Rep. Prog. Phys.* **74**, 106301 (2011).

[10] A.I. Baz, *Soviet Phys. JETP* **6**, 709 (1957); R.G. Newton, *Phys. Rev.* **114**, 1611 (1959); C. Hategan, *Ann. Phys. (NY)* **116**, 77 (1978).

[11] T. Kato, *Perturbation Theory for Linear Operators*, Springer Verlag, Berlin 1995; M.R. Zirnbauer, J.J.M. Verbaarschot, H.A. Weidenmüller, *Nucl. Phys.* **A411**, 161 (1983); W.D. Heiss, W.-H. Steeb, *J. Math. Phys.* **32**, 3003 (1991).

[12] J. Okołowicz, M. Płoszajczak, *Phys. Rev.* **C80**, 034619 (2009).

[13] J. Okołowicz, M. Płoszajczak, *Acta Phys. Pol. B* **42**, 451 (2011).

[14] B.A. Brown, W.A. Richter, *Phys. Rev.* **C74**, 034315 (2006).

[15] A.P. Zuker, B. Buck, J.B. McGrory, *Phys. Rev. Lett.* **21**, 39 (1968).
[16] F.M. Marqués *et al.*, *Phys. Rev.* **C65**, 044006 (2002).
[17] S.C. Pieper, *Phys. Rev. Lett.* **90**, 252501 (2003).
[18] C.A. Bertulani, V.G. Zelevinsky, *J. Phys. G* **29**, 2431 (2003).
[19] G. Papadimitriou *et al.*, *Phys. Rev.* **C84**, 051304(R) (2011).